arXiv:1605.06870v2 [quant-ph] 25 Oct 2016

Theory of storage and retrieval of intense-broadband pulses at room temperature: Analytical and numerical solutions

Rodrigo Gutiérrez-Cuevas*
Center for Coherence and Quantum Optics and the Institute of Optics, University of Rochester, Rochester, New York 14627, USA
(Dated: October 27, 2016)

We analyze the storage and retrieval of intense-broadband pulses with the added effects of Doppler broadening and detuning in a Λ configuration. We compute analytical solutions via the inverse scattering technique and show how the signal field is transferred to a spin-wave in the atomic medium and later retrieved by the interaction of a control pulse. Due to the intensity of the pulses, the pulse area (as defined for self-induced transparency) plays a key role in the interaction, as it determines the location of the spin wave within the medium. Additionally, we compare our results to non-ideal conditions by considering pulses of finite length and the effect of spontaneous emission.

PACS numbers: 42.50.Gy,42.50.Md,42.65.Tg,42.65.Sf

I. INTRODUCTION

The storage of light in atomic gases has its roots in photon echoes, where it was recognized that an intense π pulse could reverse the free induction decay produced by an initial pulse with arbitrary area. This inversion leads to the emission of an echo of the original pulse [1–3]. The problem with the original work was that it was conceived for a two-level system for which the transverse relaxation time is quite short, thus significantly limiting storage time. In addition, the shape of the echo is not the same as that of the stored pulse.

All these issues have been addressed throughout the years and many techniques have been proposed, most of them based on the Λ configuration (see Fig. 1). In this case, one can make the coherence between the two ground states to be long lived, thus increasing storage time. Most of the proposals are based on the phenomenon of electromagnetically induced transparency (EIT) [4], where the signal (or probe) pulse is slowed down by turning off the intense control field until it is stored in the ground states and subsequently restored by turning the control back on [5–7]. In order to avoid any significant loss due to spontaneous decay from the higher level, schemes based on stimulated Raman transitions have been proposed. Due to the high detuning, the higher atomic level can be adiabatically eliminated, which leads to simpler equations [8]. Extensions to the photon echo technique have also been worked out, where the signal pulse is mapped into a spin wave of the ground states by means of an intense π-control pulse and then retrieved by another counter-propagating strong-control pulse [9].

All these techniques address the same problem: How can we store a given signal field into an atomic medium to then retrieve it? We call this an optical memory even if the retrieved pulse is not the same as the original one: it might have a different shape, time duration, or intensity.

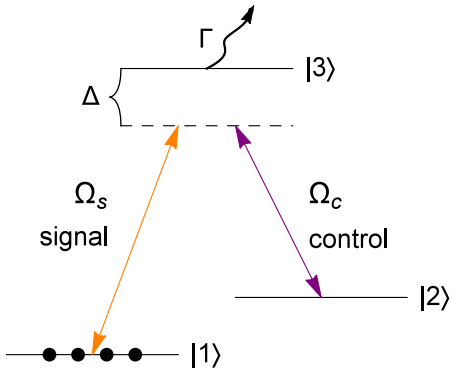

FIG. 1. (Color online) Three-level atom in Λ-configuration interacting with two fields in two-photon resonance via the common detuning Δ, with spontaneous emission Γ from the excited state.

Of course, this might not matter if we are only looking at whether a pulse is there or not. Nonetheless, the ideal scenario is the one in which the retrieved pulse is identical to the one stored (i.e., has the same shape and parameters as the original signal pulse). In any case, when one talks about optimizing these types of memories, a figure of merit must be defined. In the series of papers [10, 11] by Gorshkov *et al.* they addressed this issue by defining the efficiency as the ratio of the retrieved pulse intensity to that of the original signal pulse. Hence they can find the optimal control field to store and retrieve a given signal field by maximizing this efficiency. This work as well as that by Nunn *et al.* shows that, in general, the optimal control field has some temporal shape which differs from the usual on/off variation of the cw control used in EIT-based schemes.

Most works on pulse storage deal with a quantum (low intensity) signal pulse which allows a treatment up to first order in the signal field. There is also a recurring assumption of adiabaticity (this point has been addressed in [6, 12]) for the control pulse, and its spatial evolution is usually left out. These approximations are understand-

* rgutier2@ur.rochester.edu

able as the full set is composed of eight nonlinear partial differential equations which resist analytic solutions except in special cases [13–17]. Therefore numerical calculations are a recurring tool to study the full evolution [6, 7, 18]. In the present work, we move away from these assumptions and consider the full nonlinear equations for intense-short pulses (non-quantum and non-adiabatic fields). This is the regime of self-induced transparency (SIT), where, in a two-level system, a resonant-intense-2π pulse propagates without absorption and preserving its shape [19]. An SIT pulse can be understood as a pulse that is constantly encoding and retrieving itself resulting in a reduced group velocity.

The storage and retrieval of intense broadband pulses in a Λ system has been shown to work for cold atoms in [16, 18]. This was further extended to add more control to the information stored and the storage of multiple pulses [17]. Additionally, within the same framework, the possibility for two-channel memory and vector-pulse storage in a tripodal system has been discussed in [20]. In these works, the storage of the intense signal pulse follows a similar scheme to the one proposed in [21] for storage (a weak control pulse and intense signal pulse) but they do not discuss any retrieval procedure.

In the present work we treat the storage and retrieval of intense short pulses in the presence of Doppler broadening and detuning (this has been treated for the case of low-intensity light [11, 22]). For this, we solve the evolution equations by means of the inverse scattering transform [23, 24] for which we present an operational summary based on the work presented by Chakravarty *et al.* [24] for the particular case of a Λ system. The first and second order solutions studied show the storage and retrieval of a signal pulse while pointing towards the key parameters for this scheme, such as the pulse areas and their duration. We follow by a numerical exploration adding the effect of spontaneous emission and show that the scheme presented remains valid.

II. PHYSICAL MODEL

As was mentioned, we are looking at the storage of pulses in the characteristic regime of SIT: short (of the order of 1ns) and intense (areas around 2π) pulses. Therefore, we can omit (for the time being) the effects of spontaneous decay. We assume the atomic gas to be sufficiently dilute so as to safely neglect any loss of coherence due to collisions. Additionally, we consider that the fields are close to resonance thus validating the use of the rotating-wave approximation. Writing the fields in carrier-envelope form,

$$\begin{aligned}\boldsymbol{E}(x,t) =&\boldsymbol{\mathcal{E}}_s(x,t)e^{-i(k_s x-\omega_s t)}\\ &+\boldsymbol{\mathcal{E}}_c(x,t)e^{-i(k_c x-\omega_c t)}+c.c,\end{aligned}\tag{1}$$

we have that the Hamiltonian for the Λ-configuration (see Fig. 1) takes the form

$$\boldsymbol{H}=-\frac{\hbar}{2}\begin{pmatrix}0&0&\Omega_s\\0&0&\Omega_c\\\Omega_s^*&\Omega_c^*&-2\Delta\end{pmatrix}.\tag{2}$$

Here, we defined the Rabi frequencies for the signal and control fields, $\Omega_{s,c}(x,t)=2\boldsymbol{d}_{s,c}\cdot\boldsymbol{\mathcal{E}}_{s,c}(x,t)/\hbar$ ($d_{s,c}$ denotes the component of the dipole moment for each transition), and the detuning $\Delta=\omega_{31}-\omega_s=\omega_{32}-\omega_c$ for the two-photon resonance case.

We are interested in studying the joint evolution of the atomic system and the two fields. Hence, the equations that determine the interaction are the von Neumann equation for the atomic medium,

$$i\hbar\frac{\partial\boldsymbol{\rho}}{\partial t}=[\boldsymbol{H},\boldsymbol{\rho}],\tag{3}$$

and the wave equation in the slowly varying envelope approximation for the fields,

$$\left(\frac{\partial}{\partial x}+\frac{1}{c}\frac{\partial}{\partial t}\right)\Omega_s=-i\mu_s\langle\rho_{13}\rangle,\tag{4a}$$

$$\left(\frac{\partial}{\partial x}+\frac{1}{c}\frac{\partial}{\partial t}\right)\Omega_c=-i\mu_c\langle\rho_{23}\rangle.\tag{4b}$$

Here we defined the atom-field coupling parameters $\mu_{s,c}=N\omega_{s,c}|d_{s,c}|^2/\hbar\epsilon_0 c$ and the brackets denote the Doppler averaging,

$$\langle\rho\rangle=\int\rho(\Delta)F(\Delta)d\Delta,\tag{5}$$

over the frequency distribution

$$F(\Delta)=\frac{T_2^\star}{\sqrt{2\pi}}e^{-(\Delta-\bar{\Delta})^2T_2^{\star2}/2}\tag{6}$$

where $T_2^\star$ is the Doppler lifetime and $\bar{\Delta}$ is the mean one-photon detuning. This set of partial differential equations is referred to as the coupled Maxwell-Bloch (CMB) equations.

By further assuming equal atom-field parameters the CMB equations become integrable and can be written in the following form:

$$\frac{\partial\boldsymbol{\rho}}{\partial T}=[\boldsymbol{\Omega}-i\frac{\Delta}{2}\boldsymbol{J},\boldsymbol{\rho}]\tag{7a}$$

and

$$\frac{\partial\boldsymbol{\Omega}}{\partial Z}=\frac{\mu}{4}[\langle\boldsymbol{\rho}\rangle,\boldsymbol{J}].\tag{7b}$$

We introduced the traveling-wave coordinates $T=t-x/c$ (c being the speed of light in vacuum) and $Z=x$, and defined the matrices

$$\boldsymbol{J}=\begin{pmatrix}-1&0&0\\0&-1&0\\0&0&1\end{pmatrix},\quad\boldsymbol{\Omega}=\frac{i}{2}\begin{pmatrix}0&0&\Omega_s\\0&0&\Omega_c\\\Omega_s^*&\Omega_c^*&0\end{pmatrix}.\tag{8}$$

The integrability of the system allows the use of standard methods to find analytic solutions. Some of these methods are inverse scattering [23, 24], the Bäcklund transformation [25] and the Darboux transformation [26].

III. INVERSE SCATTERING

The method of inverse scattering allows the incorporation of Doppler broadening in a natural way for multi-pulse solutions, so we will use it to compute analytical solutions to the CMB equations instead of the Bäcklund or Darboux transformations used in previous works [14–17, 27]. In what follows, we give a pragmatic presentation of the method without going into a careful derivation of the results. We refer the interested reader to the work by Chakravarty *et al.* [24] for a complete presentation of the method for the case of a Λ system.

Since the CMB equations [Eqs. (7)] are integrable, they can be expressed as the integrability condition of the linear system

$$\frac{\partial \boldsymbol{\varphi}}{\partial T} = \left(-\frac{i\lambda}{2}\boldsymbol{J} + \boldsymbol{\Omega}\right)\boldsymbol{\varphi} \tag{9a}$$

$$\frac{\partial \boldsymbol{\varphi}}{\partial Z} = \frac{i\mu}{2}\left\langle \frac{\boldsymbol{\rho}}{\lambda - \Delta}\right\rangle \boldsymbol{\varphi}. \tag{9b}$$

That is, we recover Eqs.(7) by collecting terms with the same λ-dependence from the equation $\partial_Z\partial_T\boldsymbol{\varphi} = \partial_T\partial_Z\boldsymbol{\varphi}$. The parameter λ is referred to as the spectral parameter.

We assume the boundary conditions $\boldsymbol{\Omega} \to 0$ as $T \to \pm\infty$ for all Z, meaning the fields are composed of well-defined pulses, and fix the value of the density matrix at $T \to -\infty$ which we denote by $\boldsymbol{\rho}^{(0)}$. This, in turn, will define the final state of the atomic system $\boldsymbol{\rho}^f = \boldsymbol{\rho}(T \to \infty)$.

By integrating Eq. (9a) we can define two solutions

$$\boldsymbol{\Phi}(T,\lambda) = e^{-i\frac{\lambda}{2}\boldsymbol{J}T} + \int_{-\infty}^{T} e^{-i\frac{\lambda}{2}\boldsymbol{J}(T-T')}\boldsymbol{\Phi}(T',\lambda)\Omega(T')dT' \quad \boldsymbol{\Psi}(T,\lambda) = e^{-i\frac{\lambda}{2}\boldsymbol{J}T} + \int_{T}^{\infty} e^{-i\frac{\lambda}{2}\boldsymbol{J}(T-T')}\boldsymbol{\Psi}(T',\lambda)\Omega(T')dT' \tag{10a}$$

with the corresponding boundary conditions

$$\boldsymbol{\Phi}(T,\lambda) \to e^{-i\frac{\lambda}{2}\boldsymbol{J}T} \quad \text{as} \quad T \to -\infty \tag{11}$$

$$\boldsymbol{\Psi}(T,\lambda) \to e^{-i\frac{\lambda}{2}\boldsymbol{J}T} \quad \text{as} \quad T \to +\infty. \tag{12}$$

As these two sets of solutions determine complete sets of eigenfunctions, we can relate the two via a matrix $\boldsymbol{S}(\lambda)$ known as the scattering data,

$$\boldsymbol{\Psi} = \boldsymbol{\Phi}\boldsymbol{S}(\lambda) \quad \text{where} \quad \boldsymbol{S}(\lambda) = \begin{pmatrix} \bar{\boldsymbol{a}} & \boldsymbol{b} \\ \bar{\boldsymbol{b}}^{\dagger} & a \end{pmatrix} \tag{13}$$

with $\bar{\boldsymbol{a}}$ a 2×2 matrix and $\boldsymbol{b}$ and $\bar{\boldsymbol{b}}$ two-dimensional column vectors. It can be shown that a is analytic in the lower-half λ-plane, and we will also assume that it has a finite number of simple zeros, $\lambda_1, ..., \lambda_n$, in the region $\mathrm{Im}(\lambda) < 0$. The reflection coefficient is given by

$$\boldsymbol{r}(\lambda) = \boldsymbol{b}(\lambda)/a(\lambda) \tag{14}$$

which is well-defined on the real λ-axis.

From Eqs. (10), it is clear that the first two columns of $\boldsymbol{\Phi}$, which we denote by $\boldsymbol{\phi}$, and the last column of $\boldsymbol{\Psi}$, denoted by $\boldsymbol{\psi}$, are analytic in the lower-half λ-plane. Furthermore, they satisfy the following relation:

$$\det(\boldsymbol{\phi}, \boldsymbol{\psi}) = a(\lambda)e^{i\frac{\lambda}{2}T}. \tag{15}$$

Therefore, when evaluated at one of the simple zeros of a they become linearly dependent. Thus, we can write

$$\boldsymbol{\psi}(\lambda_j) = \boldsymbol{\phi}(\lambda_j)\boldsymbol{\eta}^{(j)}. \tag{16}$$

From this equality, we can define the norming constants, $\boldsymbol{\beta}^{(j)}$, which are written in terms of the residues of the quantity $\boldsymbol{\psi}/a$,

$$\mathrm{Res}\left\{\frac{\boldsymbol{\psi}}{a}, \lambda_j\right\} = \boldsymbol{\phi}(\lambda_j)\boldsymbol{\beta}^{(j)}, \quad \text{where} \quad \boldsymbol{\beta}^{(j)} = \frac{\boldsymbol{\eta}^{(j)}}{a'(\lambda_j)}. \tag{17}$$

In order to solve the CMB, we need to determine the evolution in Z of the scattering data (the components of the scattering matrix). This gives a number of coupled, nonlinear differential equations which, in general, do not have an analytical solution. Fortunately, the inverse scattering procedure can be carried out by simply determining the evolution of the norming constants, $\boldsymbol{\beta}^{(j)}$, and the reflection coefficient, $\boldsymbol{r}$, along with the location of the zeros of a, namely, $\lambda_1, ..., \lambda_n$. In spite of this, the general case remains an open problem. Some progress in the case of a small $\boldsymbol{r}$ has been presented in [24].

In this manuscript, we restrict ourselves to the reflection-less case, $\boldsymbol{r} = 0$. This implies that no radiation background will be superimposed to the solitonic interaction and that the initial coherences with the excited state must be zero. Therefore, the initial density matrix is block diagonal and commutes with $\boldsymbol{J}$. Thus we have

$$\boldsymbol{\rho_0}(Z,\Delta) = \begin{pmatrix} \boldsymbol{\rho_g}^{(0)}(Z,\Delta) & 0 \\ 0 & \rho_{33}^{(0)}(Z,\Delta) \end{pmatrix} \tag{18}$$

where $\boldsymbol{\rho_g}$ denotes the 2×2 density matrix of the ground state.

From Eq. (9b), the evolution of the norming constants can be derived and is given by

$$\partial_Z\boldsymbol{\beta}^{(j)} = \frac{i\mu}{2}\left\langle \frac{\boldsymbol{\rho}_g^{(0)} - \rho_{33}^{(0)}\boldsymbol{I}_2}{\lambda_j - \Delta}\right\rangle \boldsymbol{\beta}^{(j)}. \tag{19}$$

Solving this equation and using the zeros of a we can compute the fields by the following formula

$$\begin{pmatrix} \Omega_s \\ \Omega_c \end{pmatrix} = -4\sum_{j,l=1}^{n}(\boldsymbol{K}^{-1})_{jl}\alpha_l^*\boldsymbol{\beta}^{(j)}e^{i\lambda_j T} \tag{20}$$

where

$$K_{ij} = 2\frac{\alpha_i^*\alpha_j + \boldsymbol{\beta}^{(j)T}\boldsymbol{\beta}^{(i)*}e^{i(\lambda_j - \lambda_i^*)T}}{\lambda_i - \lambda_j^*} \tag{21}$$

and

$$\alpha_i = \frac{\prod_{j=1}^{n}(\lambda_j^* - \lambda_i)}{2\prod_{j\neq i}(\lambda_j - \lambda_i)}. \tag{22}$$

Likewise, we can deduce an expression for the density matrix

$$\boldsymbol{\rho} = \boldsymbol{\Phi}\boldsymbol{\rho}_0\boldsymbol{\Phi}^{-1}. \tag{23}$$

From this general expression, we can deduce a simpler formula for the density matrix for large T, i.e., after the pulses have passed, which is given by

$$\boldsymbol{\rho}^f(Z,\Delta) = \begin{pmatrix} \left(\bar{\boldsymbol{a}}^\dagger \boldsymbol{\rho_g}^{(0)} \bar{\boldsymbol{a}}\right)(\lambda=\Delta) & 0 \\ 0 & \rho_{33}^{(0)} \end{pmatrix} \tag{24}$$

with the matrix $\bar{\boldsymbol{a}}$ given by

$$\bar{\boldsymbol{a}}(\lambda) = \prod_{j=1}^{n} \boldsymbol{l}_j(\lambda), \quad \boldsymbol{l}_j(\lambda) = \boldsymbol{I}_2 + \frac{\lambda_j - \lambda_j^*}{\lambda - \lambda_j}\frac{\boldsymbol{v}^{(j)}\boldsymbol{v}^{(j)\dagger}}{\|\boldsymbol{v}^{(j)}\|^2} \tag{25}$$

where the $\boldsymbol{v}^{(j)}$ vectors are defined recursively as

$$\boldsymbol{v}^{(1)} = \boldsymbol{\beta}^{(1)}, \quad \boldsymbol{v}^{(i)} = \left(\prod_{j=1}^{i-1} \boldsymbol{l}_j(\lambda_i)\right)^{-1} \boldsymbol{\beta}^{(i)}, \quad i = 2, ..., 3. \tag{26}$$

In summary, to obtain a solution of the CMB equations (in the reflection-less case), first we need to give an initial density matrix of the form given in Eq. (18) and the spectral parameters λ_j (simple zeros of a, the number of spectral parameters determines the order of the solution). Then, we compute the evolution of the norming constants by solving Eq. (19). Finally, we use Eqs. (20-22) to obtain the evolution of the fields and Eqs. (24-26) for the final state of the atomic medium.

IV. ANALYTICAL SOLUTION

A. Pulse storage

Now that we have all the pieces to compute the solutions, we consider the particularly simple case of all the atoms prepared initially in the ground state $|1\rangle$ which is the most common situation that we encounter when dealing with EIT and pulse storage in a Λ configuration. Thus, we have

$$\boldsymbol{\rho_g}^{(0)} = \begin{pmatrix} 1 & 0 \\ 0 & 0 \end{pmatrix}, \quad \rho_{33}^{(0)} = 0. \tag{27}$$

We will start by considering the one-soliton ($n = 1$) solution and write $\lambda_1 = \xi_1 - i/\tau_1$ with $\xi_1, \tau_1 \in \Re$ and $\tau_1 > 0$. First, we solve Eq. (19) noting that the initial density matrix is independent of detuning and the matrix $\boldsymbol{\rho}_g^{(0)} - \rho_{33}^{(0)}\boldsymbol{I}_2$ is diagonal (the two equations for each component of $\boldsymbol{\beta}$ are decoupled). Thus, it is easy to see that the solution can be written as

$$\boldsymbol{\beta}^{(1)T} = \left(c_1 e^{-(\kappa_1 + i\delta_1)Z}, c_2\right) \tag{28}$$

($\boldsymbol{\beta}^{(1)T}$ denotes the transpose of $\boldsymbol{\beta}^{(1)}$) where we defined

$$\kappa_1 = \frac{\mu}{2\tau_1}\int \frac{F(\Delta)d\Delta}{(\Delta - \xi_1)^2 + (1/\tau_1)^2}, \tag{29a}$$

and

$$\delta_1 = \frac{\mu}{2}\int \frac{(\Delta - \xi_1)F(\Delta)d\Delta}{(\Delta - \xi_1)^2 + (1/\tau_1)^2}, \tag{29b}$$

with κ_1 being the absorption depth as defined for a weak-field excitation. Now, we use Eq. (20) to compute the initial pulses. Since $n = 1$ we have that $\boldsymbol{K}$ is just a scalar and $\alpha = (\lambda_1^* - \lambda_1)/2 = i/\tau_1$. Thus we obtain,

$$\begin{aligned}\Omega_s =& \frac{4c_1}{\tau_1} e^{i(\xi_1 T - \delta_1 Z)} \left[2|c_1|\cosh(T/\tau_1 - \kappa_1 Z + \sigma_1)\right. \\ &\left. + |c_2|\exp(T/\tau_1 + \kappa_1 Z + \sigma_2)\right]^{-1} \end{aligned} \tag{30a}$$

$$\begin{aligned}\Omega_c =& \frac{4c_2}{\tau_1} e^{i\xi_1 T} \left[2|c_2|\cosh(T/\tau_1 + \sigma_2)\right. \\ &\left. + |c_1|\exp(T/\tau_1 - 2\kappa_1 Z + \sigma_1)\right]^{-1} \end{aligned} \tag{30b}$$

where we defined

$$\sigma_i = \ln(|c_i|\tau_1), \quad i = 1, 2. \tag{31}$$

Therefore we see that δ_1 appears as an extra contribution to the refractive index for the signal field.

From these expressions we can calculate the pulse area for each pulse, which is defined as

$$\theta(Z) = \int_{-\infty}^{\infty} |\Omega(Z,T)|dT, \tag{32}$$

and find that the two-pulse area [15] is given by

$$\Theta(Z) = \sqrt{\theta_s(Z)^2 + \theta_c(Z)^2} = 2\pi. \tag{33}$$

This was to be expected as these are essentially the same solutions presented in [15]. At the boundary, $Z = 0$, if $|c^{(1)}| \gg |c^{(2)}|$ these are well approximated by

$$\Omega_s = \frac{\theta_s(Z=0)}{\pi\tau_1} e^{i\xi_1 T}\mathrm{sech}(T/\tau_1 + \sigma_1), \tag{34a}$$

$$\Omega_c = \frac{\theta_c(Z=0)}{\pi\tau_1} e^{i\xi_1 T}\mathrm{sech}(T/\tau_1 + \sigma_1). \tag{34b}$$

This solution describes the propagation of two matched pulses with complementing areas such that the two-pulse area is always equal to 2π. As the signal pulse propagates at a reduced group velocity, it excites some of the population to the excited state where it can be stolen by the control pulse. This leads to an amplification of the

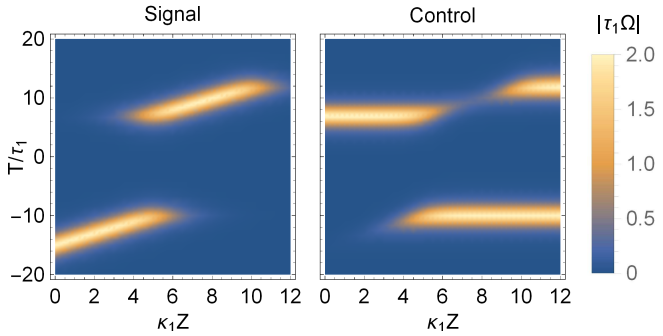

FIG. 2. (Color online) Pulse propagation as dictated by the second-order solution when $|c^{(1)}| \gg |c^{(2)}|$ and $\sigma_1 \gg \zeta$. The plot on the left (right) shows the evolution of the signal (control) pulse. For $T/\tau_1 < 0$ we have the encoding of the signal pulse onto the ground state coherence and for $T/\tau_1 > 0$ we have the retrieval followed by the re-encoding in the displaced location.

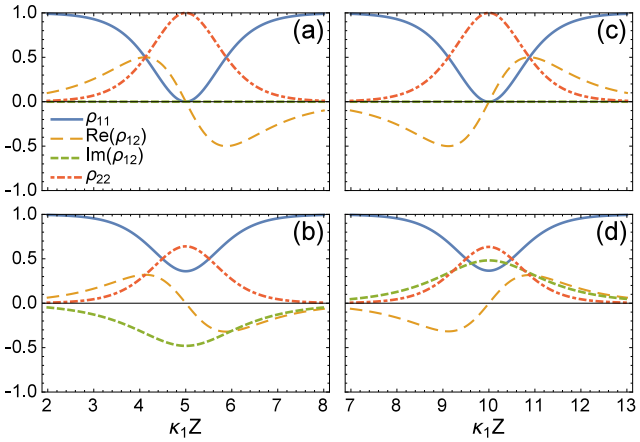

FIG. 3. (Color online) Imprint of the signal pulse in the ground state density matrix as it has been encoded before [(a) and (b)] and after the displacement [(c) and (d)]. $\tau_1\Delta = 0$ for (a) and (c) and $\tau_1\Delta = 0.75$ for (b) and (d).

control pulse while the signal pulse is absorbed. After the interaction between the two fields, the control pulse becomes a full 2π pulse propagating at the speed of light (as it is decoupled from the medium) together with the full absorption of the signal field. This is depicted in Fig. 2 for $-20 < t/\tau_1 < 0$.

Let us now take a look at the density matrix after the soliton interaction has taken place. From Eq. (24) we have that

$$\boldsymbol{\rho_g}^f(Z,\Delta) = \bar{\boldsymbol{a}}^\dagger \boldsymbol{\rho_g}^{(0)} \bar{\boldsymbol{a}} = \begin{pmatrix} |\bar{a}_{11}|^2 & \bar{a}_{11}^* \bar{a}_{12} \\ \bar{a}_{11}\bar{a}_{12}^* & |\bar{a}_{12}|^2 \end{pmatrix}. \tag{35}$$

and using Eqs. (25) and (26) we obtain

$$\bar{a}_{11}(\lambda) = 1 - \frac{i/\tau_1}{\lambda - \xi_1 + i/\tau_1}(1 - \tanh(\kappa_1 Z - \sigma_{12})), \tag{36a}$$

$$\bar{a}_{12}(\lambda) = -\frac{i/\tau_1}{\lambda - \xi_1 + i/\tau_1} C_{12} e^{-i\delta_1 Z} \mathrm{sech}(\kappa_1 Z - \sigma_{12}), \tag{36b}$$

where we defined

$$\sigma_{12} = \ln|c_1/c_2|, \quad \text{and} \quad C_{12} = \frac{c_1 c_2^*}{|c_1 c_2|}. \tag{37}$$

Finally, we can write

$$\rho_{11} = 1 + \frac{1}{\tau_1^2(\Delta - \xi_1)^2 + 1}\left[\tanh^2(\kappa_1 Z - \sigma_{12}) - 1\right], \tag{38a}$$

$$\rho_{22} = \frac{1}{\tau_1^2(\Delta - \xi_1)^2 + 1}\mathrm{sech}^2(\kappa_1 Z - \sigma_{12}), \tag{38b}$$

$$\rho_{12} = -\frac{C_{12} e^{-i\delta_1 Z}}{\tau_1^2(\Delta - \xi_1)^2 + 1}\left[i\tau_1(\Delta - \xi_1) + \tanh(\kappa_1 Z - \sigma_{12})\right] \times \mathrm{sech}(\kappa_1 Z - \sigma_{12}). \tag{38c}$$

From these equations it is clear that while the switching between the signal and control pulses is taking place, the signal pulse is being transferred into a spin wave (imprint) located at $\kappa_1 Z = \sigma_{12}$. This location, denoted x_1, can be written in terms of the pulse area to give the simple formula

$$\kappa_1 x_1 = \ln\left(\frac{\theta_s(Z=0)}{\theta_c(Z=0)}\right). \tag{39}$$

Hence, the ratio of the pulse areas plays a key role during the storage of the signal pulse as it determines the location of the imprint. Figures 3(a) and (b) show the shape of the imprint for two different detuning values. The storage procedure is in line with the proposal made in [21], where an intense pulse is mapped into a spin wave by means of a low-intensity control pulse in order to reduce the storage length as compared to the usual EIT techniques. Yet, no mention of a retrieval procedure was made, and so we address this point in the next section.

B. Pulse retrieval and spin wave manipulation

Having analyzed in detail how an intense pulse can be mapped into a spin wave, we need to address the matter of retrieving the information stored. Looking at previous work on the subject, we see that in order to recover the signal pulse we need to apply a control field. Going back to the first-order solution we notice that if we set the integration constant c_1 in (28) equal to zero, the norming constant is given by

$$\boldsymbol{\beta}^{(2)T} = (0, d). \tag{40}$$

This leads to a 2π-control field propagating at the speed of light in vacuum

$$\Omega_c = \frac{2}{\tau_2}\frac{d}{|d|} e^{i\xi_2 T}\mathrm{sech}(T/\tau_2 + \zeta), \tag{41}$$

where the spectral parameter was taken to be $\lambda_2 = \xi_2 - i/\tau_2$ and we defined

$$\zeta = \ln(|d|\tau_2). \tag{42}$$

To study how this control pulse interacts with the spin wave encoded in the medium, we compute the second-order ($n = 2$) solution obtained from the norming constants as defined in Eqs. (28) and (40), and the two spectral parameters λ_1 and λ_2. Using Eqs. (20) through (22) we obtain an exact solution which is too cumbersome to be of any use. Hence, we look at the limiting case of $|c^{(1)}| \gg |c^{(2)}|$ and $\sigma_1 \gg \zeta$ for which the pulses at the boundary $Z = 0$ can be well approximated by

$$\begin{aligned}\Omega_s =&\frac{2}{\tau_1}\frac{c_1}{\sqrt{|c_1|^2+|c_2|^2}}e^{i\xi_1 T}\mathrm{sech}(T/\tau_1+\sigma_1)\\ &+\frac{2}{\tau_2}\frac{c_2}{\sqrt{|c_1|^2+|c_2|^2}}e^{i\xi_2 T}\mathrm{sech}(T/\tau_2+\zeta-\chi),\end{aligned} \tag{43a}$$

$$\begin{aligned}\Omega_c =&\frac{2}{\tau_1}\frac{c_2}{\sqrt{|c_1|^2+|c_2|^2}}e^{i\xi_1 T}\mathrm{sech}(T/\tau_1+\sigma_1)\\ &+\frac{2}{\tau_2}\frac{c_1}{\sqrt{|c_1|^2+|c_2|^2}}e^{i\xi_2 T}\mathrm{sech}(T/\tau_2+\zeta-\chi),\end{aligned} \tag{43b}$$

where we defined the phase-lag parameter

$$\chi = \frac{1}{2}\ln\left(\frac{(\tau_1+\tau_2)^2+(\xi_1-\xi_2)^2\tau_1^2\tau_2^2}{(\tau_1-\tau_2)^2+(\xi_1-\xi_2)^2\tau_1^2\tau_2^2}\right). \tag{44}$$

This expression describes a well-defined sequence of pulses. First, we have the matched pulses of duration τ_1 that encode the strong signal pulse into the medium. These have the same form as the pulses in Eq. (34) and thus lead to the storage of the signal pulse at a location determined by Eq. (39). Then we have another set of matched pulses but of duration τ_2 and inverted areas, that is, we have a strong control pulse and a weak signal pulse having the same areas as the initial storing set. This solution is shown in Fig. 2, where we can clearly see that initially we have the same type of solution described in the previous section followed by the interaction of the second set of matched pulses with the spin wave left by the first. As the pulses approach the location of the imprint, the signal pulse is amplified at the expense of the control pulse up to the point where it becomes a full 2π pulse (here we can say that the signal pulse is retrieved). After propagating a given distance, we have another reversal of intensities: the signal pulse is absorbed leading to the amplification of the control pulse which, after becoming a full 2π pulse, becomes decoupled from the medium.

There are two main points to mention as far as the usual concept of pulse storage and retrieval. First, the retrieved pulse does not have the same properties as the original signal pulse if the spectral parameters differ. The retrieval would, of course, be achieved by cutting off the medium at the location where the signal pulse has maximum intensity. Second, the retrieval control pulse is not just a control field but is accompanied by the same amount of signal field as there was of the control field for the storage. This contrasts with the usual distinction of one frequency controlling the other. We will study how this compares with just using a 2π control field for the retrieval in Sec. V.

Now let us take a look at the density matrix after the interaction of the second matched pulse set with the spin wave left behind by the first. For this, we again use Eqs. (25) and (26) to obtain the following expressions for scattering coefficients:

$$\bar{a}_{11}(\lambda) = 1 - \frac{i/\tau_1}{\lambda-\xi_1+i/\tau_1}(1-\tanh(\kappa_1 Z-\sigma_{12}-\chi)), \tag{45a}$$

$$\bar{a}_{12}(\lambda) = -\frac{i/\tau_1}{\lambda-\xi_1+i/\tau_1}C_{12}e^{-i\delta Z}e^{i\phi}\mathrm{sech}(\kappa_1 Z-\sigma_{12}-\chi), \tag{45b}$$

where the extra phase ϕ depends on the two eigenvalues λ_1 and λ_2. When these are purely imaginary, $\phi = \pi$. As a result, the density matrix takes the form

$$\rho_{11} = 1 + \frac{1}{\tau_1^2(\Delta-\xi)^2+1}\left[\tanh^2(\kappa_1 Z-\sigma_{12}-\chi)-1\right], \tag{46a}$$

$$\rho_{22} = \frac{1}{\tau_1^2(\Delta-\xi)^2+1}\mathrm{sech}^2(\kappa_1 Z-\sigma_{12}-\chi), \tag{46b}$$

$$\begin{aligned}\rho_{12} =&\frac{-C_{12}e^{-i\delta Z}e^{i\phi}}{\tau_1^2(\Delta-\xi)^2+1}\left[i\tau_1(\Delta-\xi)+\tanh(\kappa_1 Z-\sigma_{12}-\chi)\right]\\ &\times\mathrm{sech}(\kappa_1 Z-\sigma_{12}-\chi).\end{aligned} \tag{46c}$$

These have the same form as those given in Eqs. (38), and so the result of the interaction with the second set is clear: the spin wave has been displaced by an amount determined by the phase-lag parameter χ. Additionally, the coherence suffered a ϕ phase shift. Therefore, if the medium is not cut off before the retrieved pulse is absorbed, the imprint is displaced further into the medium with new location

$$\kappa_1 x_2 = \sigma_{12} + \chi. \tag{47}$$

C. Effects of Doppler broadening and detuning

Let us take a moment to study the effect of inhomogeneous broadening and detuning in the solutions just described. Tracing back our steps, we readily notice that the only place where a Doppler average is taken is in Eqs. (29). From the expressions for the pulses and the spin-wave it is clear that the absorption coefficient sets the spatial dimension, that is, the smaller κ_1 is, the longer the atomic sample will need to be in order to fit the pulses and the spin-wave. On the other hand, the only effect

of the parameter δ_1 is to produce a position-dependent phase to the signal pulse which is in turn transferred to the spin-wave.

So far we have kept the spectral parameters complex, but taking a look at the expression for the pulses [Eqs. (30) and (43)] we notice that the imaginary part can be identified as the pulse duration while the real part appears as a self-detuning term. This term also appears in the expression for κ_1 and δ_1 by shifting the detuning everywhere except in the Doppler distribution. Furthermore, looking back at the definition of the Rabi frequencies and the slow-varying envelopes for the fields, we see that this self-detuning should be included as a real detuning. Thus we set it to zero and rewrite the expressions for κ_1 and δ_1 in term of the absorption coefficient in the absence of Doppler broadening, $\kappa_0 = \mu\tau_1/2$,

$$\kappa_1 = \kappa_0 \int \frac{\bar{F}(\nu)d\nu}{\nu^2+1}, \tag{48a}$$

$$\delta_1 = \kappa_0 \int \frac{\nu\bar{F}(\nu)d\nu}{\nu^2+1}, \tag{48b}$$

where

$$\bar{F}(\nu) = \frac{T_2^\star}{\tau\sqrt{2\pi}} e^{-(\nu-\tau\bar{\Delta})^2 T_2^{\star 2}/2\tau^2}. \tag{49}$$

We plot these as a function of the Doppler distribution width and mean (see Fig. 4). We readily notice that the maximum value for the absorption coefficient is attained in the absence of Doppler broadening and zero detuning. When the detuning is non-zero, the maximum for κ shifts to a wider Doppler distribution. As the absorption coefficient sets the spatial length, this can be used to reduce the size of the atomic sample if detuning is unavoidable. As for the extra contribution to the index of refraction, there must be some detuning in order for it to have some effect due to the anti-symmetry of δ_1 with respect to $\bar{\Delta}$. Moreover, both parameters tend to zero in the limits of large width and detuning, so in general it is preferable to keep them as low as possible to reduce the size of the atomic sample.

The absorption coefficient also determines the group velocity of the signal pulse, which is given by

$$\frac{v_g}{c} = \frac{1}{1+\kappa_1 c\tau}. \tag{50}$$

Hence, as κ becomes smaller the signal pulse travels faster through the medium and so needs to interact for a larger distance with the medium to be able to produce the same effect as a slower pulse. This is in clear accordance with the previous discussion about how κ sets the spatial dimension. The change in spatial dimension is also present in the expressions for the location of the initial imprint and the displacement which can be written as

$$\kappa_0 x_1 = \frac{\kappa_0}{\kappa_1} \ln\left(\frac{\theta_s(Z=0)}{\theta_c(Z=0)}\right), \tag{51a}$$

$$\kappa_0 \Delta x = \kappa_0(x_2 - x_1) = \frac{\kappa_0}{\kappa_1} \ln\left(\frac{\tau_1+\tau_2}{\tau_1-\tau_2}\right). \tag{51b}$$

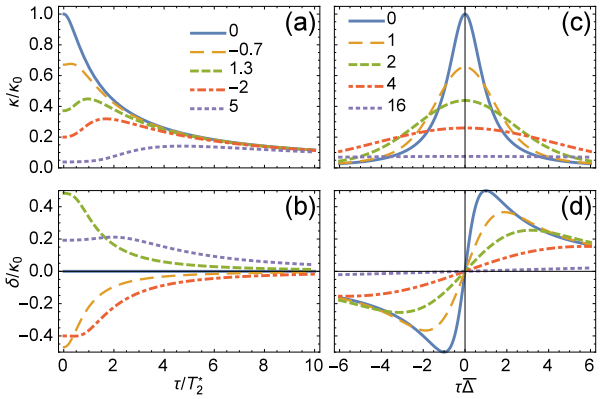

FIG. 4. (Color online) Absorption coefficient κ and extra contribution to the index of refraction δ as a function of the Doppler width and mean detuning. (a) shows κ and (b) δ as a function of τ/T_2^* for $\tau\bar{\Delta} = 0, -0.6, 1.2, -2, 5$. (c) shows κ and (d) δ as a function of $\tau\bar{\Delta}$ for $\tau/T_2^* = 0, 1, 2, 4, 16$.

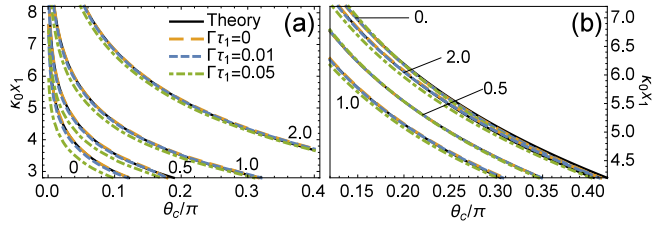

FIG. 5. (Color online) Location of the stored spin wave as a function of the control pulse area for (a) $\tau\bar{\Delta} = 0$ and $\tau/T_2^* = 0, 0.5, 1, 2$ and (b) $\tau\bar{\Delta} = 1.3$ and $\tau/T_2^* = 0, 0.5, 1, 2$.

V. NON-IDEAL PULSE STORAGE AND RETRIEVAL

After discussing the analytic solution in detail we need to compare it to more realistic conditions. In order to accomplish this we recur to numerical calculations. Note that the initial assumption of zero decay was justified since the lifetime of the higher level is around two orders of magnitude longer that the duration of the pulses for the regime in which we are working. As an example, for Rb we have $\tau\Gamma \approx 0.01$ for pulse duration $\tau \approx 0.26$ns [28]. We will consider it, as well as the finiteness of the pulses, as it may have a noticeable effect. We will assume that the decay rate into each ground state is the same for a given decay rate Γ for the excited state. Additionally, we set the Rabi frequencies equal to zero when $|\tau_1\Omega| < 10^{-5}$.

First, we consider the storage of the signal pulse and thus the location of the stored spin-wave. The results for different values of the parameters are shown in Fig. 5. We notice that it is difficult to distinguish between the different curves, but that is due to the agreement between the analytical solution and the numerical results. In the absence of detuning [Fig. 5(a)] we note that the effect of spontaneous emission is to lower the curve, that is, the signal pulse is stored before the predicted location. This

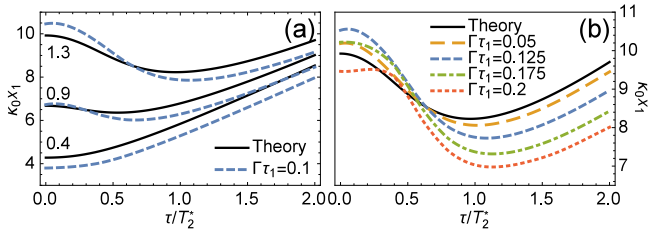

FIG. 6. (Color online) Location of the stored spin wave as a function of the Doppler width for a control pulse area of $\theta_c = 0.05\pi$. In (a) we fix the decay rate and consider different values for the detuning, $\tau\bar{\Delta} = 0.4, 0.9, 1.3$ and in (b) we fix the detuning at $\tau\bar{\Delta} = 1.3$ and vary the decay rate.

is the same effect that was reported in [18] in the absence of Doppler broadening.

If we now take a closer look at Fig. 5(b) we can spot some differences. The most noticeable effect is that the curves have been reversed. In this case ($\tau\bar{\Delta} = 1.3$) the spin wave for a Doppler width of $\tau/T_2^* = 0.5$ is located after the one made for $\tau/T_2^* = 1$. This is just a consequence of the displaced maximum for κ_1 as a function of the width [see Fig. 4(a)]. In addition there is a somewhat hidden feature. For a Doppler width of $\tau/T_2^* = 0.5$ the effect of spontaneous emission is suppressed: the four curves overlap almost perfectly. While for $\tau/T_2^* = 0$ the effect is reversed. As for the other two width values, the curves with spontaneous emission are lowered, but for $\tau/T_2^* = 1$ the effect is less noticeable.

To investigate this strange phenomenon we plot the location of the imprint as a function of T_2^* for a higher value of spontaneous emission $\tau\Gamma = 0.1$ [see Fig. 6(a)]. The effect is clear: for sufficiently detuned fields the effect of spontaneous emission is reversed for small values of the Doppler width. Now, with increasing rate of spontaneous emission, the reversal is enhanced until it reaches a maximum [see Fig. 6(b)]. After this, the effect is diminished. Comparing the crossing of the numerical results with the curve predicted by the theory we notice that this reversal is limited to the region where $\partial\kappa/\partial(\tau/T_2^*) > 0$. This effect is independent of the sign of the detuning.

Now, let us take a look at the displacement of the spin-wave. We show the results for different values of Doppler width, detuning and spontaneous decay rate along with the theoretical result in Fig. 7. We notice that in the absence of spontaneous emission the numerical results are very similar to those predicted by the analytical solution. The only difference is that the maximum displacement is attained for values slightly bigger than $\tau_2 = \tau_1$. The biggest deviation is when $\tau\bar{\Delta} = 1.3$ and $\tau/T_2^* = 2$ [see Fig. 7(h)], which is also the case where the largest control-pulse area is required for the storage of the 2π-signal pulse and thus is the one where the two-pulse area deviates the most from the one predicted for the storage stage.

The effect of spontaneous emission is evident: as the decay rate increases, the maximum displacement is

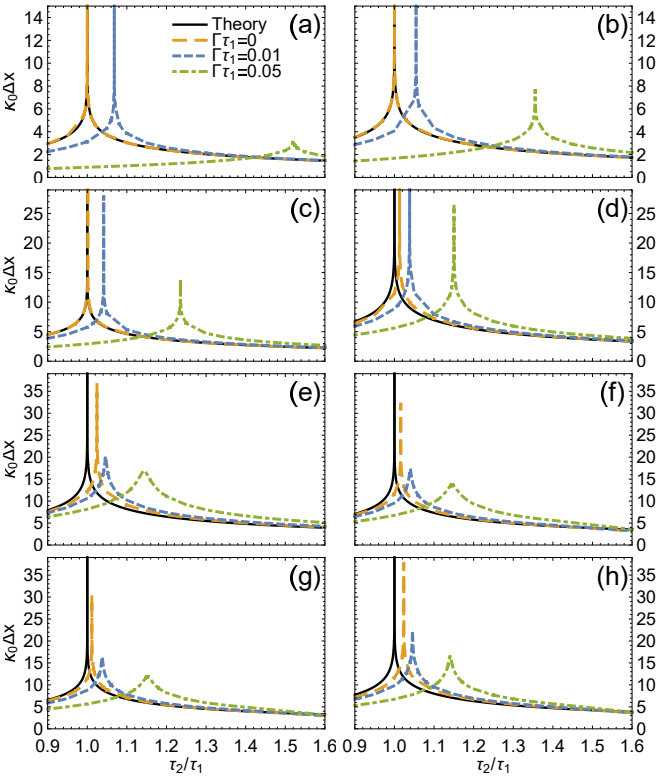

FIG. 7. (Color online) Displacement of the stored spin wave as a function of the second control pulse duration for $\tau\bar{\Delta} = 0$ and (a) $\tau/T_2^* = 0$, (b) $\tau/T_2^* = 0.5$, (c) $\tau/T_2^* = 1$ and (d) $\tau/T_2^* = 2$. Then we fix $\tau\bar{\Delta} = 1.3$ and (e) $\tau/T_2^* = 0$, (f) $\tau/T_2^* = 0.5$, (g) $\tau/T_2^* = 1$ and (h) $\tau/T_2^* = 2$. The initial location of the imprint was chosen to be at $\kappa_0 x_1 = 5$ where the storage was made by a 2π-signal pulse and the required control pulse.

shifted to larger values of τ_2. This is coupled with a lowering in the maximum displacement with increasing rate of spontaneous emission: For the cases with no detuning and spontaneous decay $\tau\Gamma \leq 0.01$, by using double precision numbers, no maximum was attained but we can be fairly certain that a maximum should be attained at least for the cases with non-zero decay because of the pulse dynamics shown in Fig. 8 as explained in the next paragraph. Here, there is a clear difference between the cases with spontaneous emission and the one without, unlike in the storage stage. Nonetheless, a considerable displacement of the spin-wave can be achieved in each case as long as the right duration for the control pulse is chosen (this feature was not reported in [18] as the duration of the control pulses was always lower than that of the original signal pulse).

Figure 8 shows the pulse dynamics in the retrieval stage at the displacement peaks for the cases in resonance with $\tau/T_2^* = 1$. We only show one value for the Doppler broadening width as the other cases behave in the same way. Let us first take a look at the case in resonance. The first thing we notice is that for the case with no decay, the retrieval behaves pretty much as described by

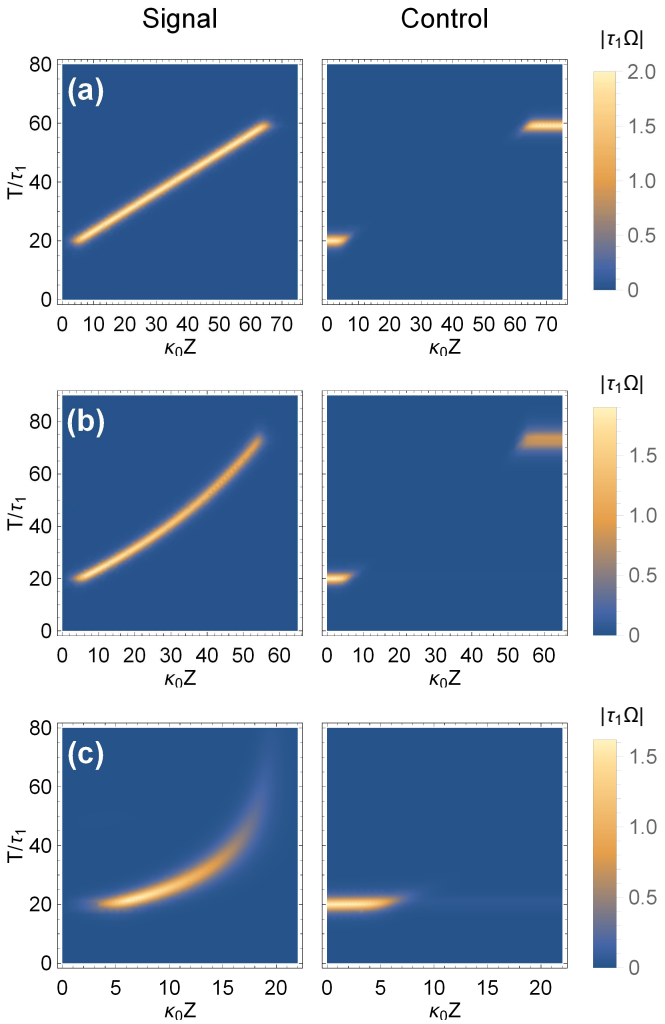

FIG. 8. (Color online) Pulse dynamics around the displacement peaks for $\tau\bar{\Delta} = 0$ and (a) $\tau\Gamma = 0$, (b) $\tau\Gamma = 0.01$, and (c) $\tau\Gamma = 0.05$.

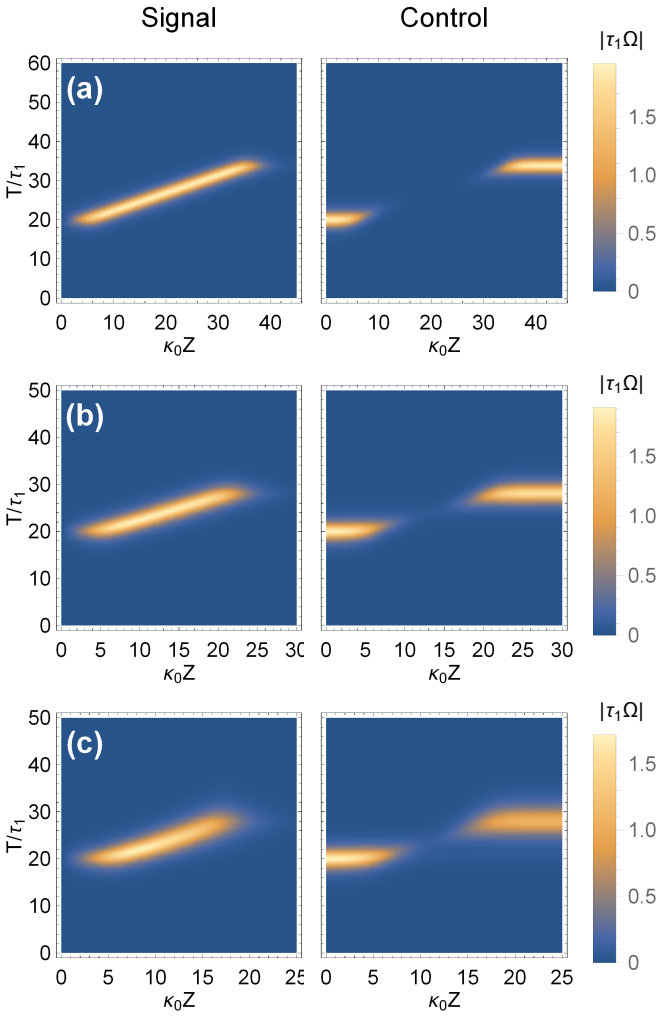

FIG. 9. (Color online) Pulse dynamics around the displacement peaks for $\tau\bar{\Delta} = 1.3$ and (a) $\tau\Gamma = 0$, (b) $\tau\Gamma = 0.01$, and (c) $\tau\Gamma = 0.05$.

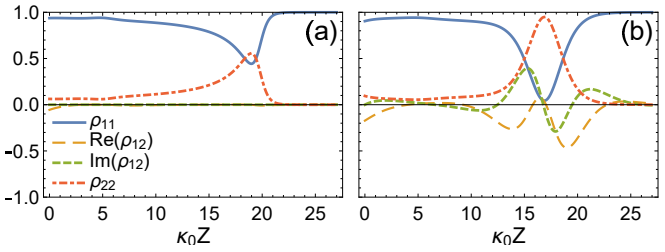

FIG. 10. (Color online) Density matrix elements for the ground states after the maximum displacement for $\tau\Gamma = 0.05$ and (a) $\tau\bar{\Delta} = 0$ and (b) $\tau\bar{\Delta} = 1.3$.

the analytical solution. Now, if we add some decay channel we notice that the signal pulse starts slowing down at the same time as it decays. For the case with highest spontaneous emission the signal pulse almost comes to a full stop, as can be understood by the close to 90 degrees turn. As for the case with $\tau\Gamma = 0.01$, the slowing down and decay are evidence of the eventual maximum displacement which was not achieved due to limitations in the precision. If we now go off resonance (see Fig. 9) we notice that the slowing down disappears. This can be a result of the reduced population induced in the excited state. Another consequence of this is the preservation of the coherence between the ground state levels which would allow another retrieval. Figure 10 shows the density matrix elements for the cases with $\tau\Gamma = 0.05$. We readily notice that the coherence is completely lost when in resonance whilst it is mostly preserved in the detuned scenario. Therefore, the detuning prevents the loss of coherence due to spontaneous emission. It is also worth noting that a maximum displacement is always attained even for the case with no decay channel.

Moving on to the retrieval of the signal pulse we find that there is a caveat, though. As we already mentioned in the analytical solution, the retrieved signal pulse inherits the duration of the control pulse used to retrieve

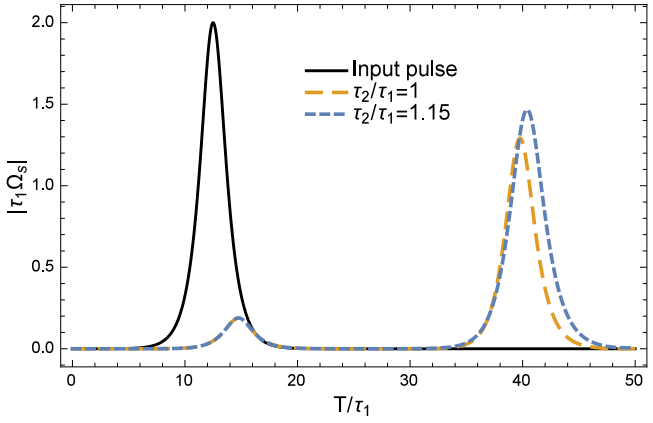

FIG. 11. (Color online) Input 2π-signal pulse ($\kappa_0 Z = 0$) and output pulses ($\kappa_0 Z = 10$) for two values of the duration of the control pulse $\tau_2/\tau_1 = 1, 1.15$. The atomic medium is ten κ_0^{-1} long and we chose $\tau\bar{\Delta} = 0$, $\tau/T_2^* = 2$ and $\tau_1\Gamma = 0.05$.

it. This remains true in the non-idealized scenario as can be seen in Fig. 11. Therefore there is a compromise: if we want the highest output intensity then we have to allow the duration of the retrieved pulse to be different or, conversely, if we want to keep the same parameters for the signal pulse we will have to settle for a lower output intensity. In this regard, the presence of Doppler broadening and detuning helps by bringing the maximum displacement closer to that predicted by the theory.

As a last note, this scheme also helps reduce the storage length compared to the usual EIT scheme. This was also noted in [21]. For the parameters considered in this work the EIT-type interaction has a minimal effect in both the control and signal fields for the equivalent distances considered here. These need to be substantially increased in order to see the formation of the adiabaton pair [13].

VI. CONCLUSIONS

In conclusion, we have used the technique of inverse scattering to obtain analytical solutions that describe the storage and retrieval of intense pulses in the presence of Doppler broadening and detuning. These results are in accordance with previous treatments [16, 18]. Only minor corrections are needed and the main effect (according to analytical solutions) is the change in length scale which is determined by κ_1, thus showing that the preliminary conjectures made in [17] were somewhat pessimistic.

Additionally, we have tested the result given by the analytical solution via numerical solutions through which we have found a notable agreement for the storage step. The addition of homogeneous broadening causes a minimal deviation from the theoretical predictions and a strange reversal of its effect in the region where $\partial\kappa/\partial(\tau/T_2^*) > 0$. As for the displacement (or retrieval, if the displacement is greater than the medium length), the differences with the theory are appreciable but nonetheless follow a similar trend. Most noticeable is the shift of the maximum for the displacement of the spin-wave (an effect previously overlooked) which would allow the experimental realization of this procedure even for higher values of decay rate. It is also worth highlighting the slowing down of the retrieved pulse when in resonance (due to the spontaneous decay) and its disappearance, along with the protection of coherence as we go off-resonance.

The results presented here and in [18] show that this storage scheme can be implemented experimentally in a variety of conditions. In addition, the backward-transfer solution as well as the multi- pulse storage presented in [17] should remain valid with the appropriate change of the spatial dimension.

ACKNOWLEDGMENTS

The author gratefully acknowledges J. H. Eberly and M. A. Alonso for fruitful discussions and a careful review of this manuscript. This work was supported by NSF grants (PHY-1203931, PHY-1505189) and a CONACYT fellowship awarded to R. Gutiérrez-Cuevas.

[1] E. L. Hahn, Phys. Rev. **80**, 580 (1950).
[2] N. Kurnit, I. Abella, and S. Hartmann, Phys. Rev. Lett. **13**, 567 (1964).
[3] T. W. Mossberg, Opt. Lett. **7**, 77 (1982).
[4] S. E. Harris, Phys. Today **50**, 36 (1997); K.-J. Boller, A. Imamoğlu, and S. E. Harris, Phys. Rev. Lett. **66**, 2593 (1991).
[5] M. Fleischhauer and M. D. Lukin, Phys. Rev. Lett. **84**, 5094 (2000).
[6] A. B. Matsko, Y. V. Rostovtsev, O. Kocharovskaya, A. S. Zibrov, and M. O. Scully, Phys. Rev. A **64**, 043809 (2001).
[7] T. N. Dey and G. S. Agarwal, Phys. Rev. A **67**, 033813 (2003).
[8] J. Nunn, I. A. Walmsley, M. G. Raymer, K. Surmacz, F. C. Waldermann, Z. Wang, and D. Jaksch, Phys. Rev. A **75**, 011401 (2007); K. F. Reim, P. Michelberger, K. C. Lee, J. Nunn, N. K. Langford, and I. A. Walmsley, Phys. Rev. Lett. **107**, 053603 (2011).
[9] S. A. Moiseev and S. Kröll, Phys. Rev. Lett. **87**, 173601 (2001).
[10] A. V. Gorshkov, A. André, M. Fleischhauer, A. S. Sørensen, and M. D. Lukin, Phys. Rev. Lett. **98**, 123601 (2007); A. V. Gorshkov, A. André, M. D. Lukin, and

A. S. Sørensen, Phys. Rev. A **76**, 033804 (2007); **76**, 033805 (2007); A. V. Gorshkov, T. Calarco, M. D. Lukin, and A. S. Sørensen, **77**, 043806 (2008).
[11] A. V. Gorshkov, A. André, M. D. Lukin, and A. S. Sørensen, Phys. Rev. A **76**, 033806 (2007).
[12] R. N. Shakhmuratov, A. A. Kalachev, and J. Odeurs, Phys. Rev. A **76**, 031802 (2007).
[13] R. Grobe, F. T. Hioe, and J. H. Eberly, Phys. Rev. Lett. **73**, 3183 (1994).
[14] Q. Han Park and H. J. Shin, Phys. Rev. A **57**, 4643 (1998).
[15] B. D. Clader and J. H. Eberly, Phys. Rev. A **76**, 053812 (2007).
[16] E. Groves, B. D. Clader, and J. H. Eberly, J. Phys. B: At. Mol. Opt. Phys. **46**, 224005 (2013).
[17] R. Gutiérrez-Cuevas and J. H. Eberly, J. Opt. Soc. Am. B **32**, 2271 (2015).
[18] R. Gutiérrez-Cuevas and J. H. Eberly, Phys. Rev. A **92**, 033804 (2015).
[19] S. L. McCall and E. L. Hahn, Phys. Rev. Lett. **18**, 908 (1967); Phys. Rev. **183**, 457 (1969).
[20] R. Gutiérrez-Cuevas and J. H. Eberly, Phys. Rev. A **94**, 013820 (2016).
[21] G. Grigoryan, Y. Pashayan-Leroy, C. Leroy, and S. Guerin, Phys. Rev. A **79**, 013813 (2009).
[22] N. Sangouard, C. Simon, M. Afzelius, and N. Gisin, Phys. Rev. A **75**, 032327 (2007).
[23] C. S. Gardner, J. M. Greene, M. D. Kruskal, and R. M. Miura, Phys. Rev. Lett. **19**, 1095 (1967); M. J. Ablowitz, D. J. Kaup, A. C. Newell, and H. Segur, **31**, 125 (1973); G. L. Lamb, *Elements of Soliton Theory* (Wiley, New York, 1980).
[24] S. Chakravarty, B. Prinari, and M. Ablowitz, Physica D **278**, 58 (2014).
[25] G. L. Lamb, Rev. Mod. Phys. **43**, 99 (1971); R. M. Miura, *Backlund Transformations* (Springer-Verlag, Berlin, 1976); Q.-H. Park and H. J. Shin, Phys. Rev. A **57**, 4621 (1998).
[26] C. Gu, H. Hu, and Z. Zhou, *Darboux Transformations in Integrable Systems* (Springer, Dordrecht, 2005); J. L. Cieśliński, J. Phys. A: Math. Theor. **42**, 404003 (2009).
[27] B. D. Clader and J. H. Eberly, Phys. Rev. A **78**, 033803 (2008).
[28] D. A. Steck, "Rubidium 87 D Line Data," available online at http://steck.us/alkalidata (revision 2.1.4, 23 December 2010).